Lack of Hypoxic Response in Uterine Leiomyomas despite Severe Tissue Hypoxia

Arnulf Mayer,[1] Michael Höckel,[2] Alexander Wree,[1] Cornelia Leo,[2] Lars-Christian Horn,[3] and Peter Vaupel[1]

[1]Institute of Physiology and Pathophysiology, Johannes Gutenberg University, Mainz, Germany and [2]Department of Gynecology and Obstetrics, University of Leipzig Medical Center and [3]Department of Pathology, University of Leipzig, Leipzig, Germany

Abstract

Hypoxia is now established as a key factor influencing the pathophysiology of malignant growth. Among other effects, hypoxia modulates the expression of a multitude of genes through the induction of hypoxia-inducible transcription factors. This differential gene expression favors angiogenesis, cell survival, an invasive/metastatic phenotype, and resistance to anticancer therapies. Because benign tumors do not exhibit these traits, one might expect these entities to be neither hypoxic nor to induce the genetic hypoxia response program. To test this hypothesis, an investigation of the oxygenation status of 17 leiomyomas and 1 leiomyosarcoma of the uterus using polarographic needle electrodes (Eppendorf pO_2 sensor) and the expression of hypoxia-related markers in biopsy specimens of the same tumors was carried out. Marker expression in eight additional archival leiomyosarcomas was also assessed. Leiomyoma tissue was generally found to be severely hypoxic, with median oxygen (O_2) partial pressure values ranging from 1 to 5 mm Hg. In contrast, none of the hypoxia-related markers hypoxia-inducible factor (HIF)–1α, HIF-2α, glucose transporter-1, or carbonic anhydrase IX were expressed in any leiomyoma. Larger intercapillary distances were correlated with a poorer oxygenation status. Conversely, the expression of hypoxia-related markers was abundant in the leiomyosarcomas and they also exhibited a high-turnover phenotype (significantly increased proliferation and apoptosis). Uterine leiomyoma might therefore represent a state of oxygen-limited proliferation. Malignancy in the same organ system is associated with growth and metabolism beyond tissue-inherent limitations leading to the induction of hypoxia-related markers, thereby contributing to a self-perpetuating aggressive phenotype. [Cancer Res 2008;68(12):4719–26]

Introduction

Earlier clinical investigations in various tumor entities, such as head and neck cancer, cervical cancer, and soft tissue sarcoma found a correlation between tumor oxygenation and prognosis irrespective of the treatment modality used (1–4). These results gained considerable attention in the field of cancer research and therapy because they pointed to a new clinically applicable "universal" indicator of tumor aggressiveness and paved the way for further insights into the pathobiology ("pathophysiome") of malignant disease (5–9). The notion of tumor hypoxia presenting an obstacle to the success of radiotherapy and some forms of chemotherapy shifted to the notion of tumor hypoxia as an important driving force in malignant progression (10). Further findings revealed that hypoxia—as an inherent consequence of unregulated tissue growth—promotes local invasion, intravasation, and finally metastatic spread at three levels and that this occurs in a cooperative manner: (*i*) on the proteome/metabolome level through adaptive gene expression, posttranscriptional, and post-translational modifications; (*ii*) on the genome/epigenome level by increasing genomic and epigenomic instability; and (*iii*) on the level of cell populations by selection and clonal expansion according to phenotype fitness (11, 12).

Hypoxia-induced changes in gene expression (*level i*) are coordinated mainly by the hypoxia-inducible factor-1 (HIF-1) and HIF-2 (13, 14). Downstream effects of HIF activation, which contribute to increased malignancy, include modulation of glucose metabolism through increased cellular glucose uptake via glucose transporter-1 (GLUT-1) and enhanced glycolysis by up-regulation of key glycolytic enzymes, increased proton-extrusion capacity (15) by overexpression of carbonic anhydrase IX (CA IX), increased angiogenesis by up-regulation of vascular endothelial growth factor, and the activation of the c-MET/HGF system characterized by cell proliferation, cell-cell dissociation, migration, and apoptosis protection.

Sporadic uterine leiomyomas are the most frequent benign tumors in women, arising in 40% to 70% of all women in their later reproductive years. Solitary or multiple leiomyomas originate predominantly from smooth muscle cells of the myometrium. They are estrogen-dependent, relatively slow-growing tumors derived from single-cell clones generated independently without invasive and metastatic features (16). Their malignant counterparts, i.e., leiomyosarcomas, are diagnosed in <0.5% of surgically treated mesenchymal uterine tumors and are regarded as being unrelated to sporadic benign leiomyomas (17, 18). Despite long phases of autonomous growth, which may result in large tumors, uterine leiomyomas exhibit no clinically significant tendency for invasion or metastasis. Thus, according to the aforementioned pathophysiologic model, these lesions would not be expected to be hypoxic and elements of the transcriptional response evoked by HIFs should be inactive.

To test this hypothesis, tumor oxygenation profiles were measured and analyzed and four key markers of the HIF response (HIF-1α, HIF-2α, GLUT-1, and CA IX), proliferation (Ki-67), apoptosis [terminal deoxynucleotidyl transferase (TdT)–mediated dUTP nick-end labeling (TUNEL) assay], and intercapillary distance (ICD; image analysis of CD34/CD31 staining) were determined in proliferating uterine leiomyoma. Marker expression was also

Note: Supplementary data for this article are available at Cancer Research Online (http://cancerres.aacrjournals.org/).

Requests for reprints: Arnulf Mayer, Institute of Physiology and Pathophysiology, University of Mainz, Duesbergweg 6, 55128 Mainz, Germany. Phone: 49-6131-39-25929; Fax: 49-6131-39-25774; E-mail: arnmayer@uni-mainz.de.

doi:10.1158/0008-5472.CAN-07-6339

analyzed in normal myometrium and in the malignant counterpart (leiomyosarcoma). However, due to the extreme rarity of this latter entity, oxygenation data were only available for one sarcoma.

Materials and Methods

Patients, pO_2 measurement, and tissue specimens. All patients were part of a prospective clinical study evaluating the significance of intratumoral hypoxia in benign and malignant uterine tumors that took place from 2001 to 2005 at the Department of Gynecology and Obstetrics of the University of Leipzig Medical Center. Intratumoral oxygen tension (pO_2) measurement was performed with the Eppendorf histography system (Eppendorf) according to the standard procedure first described in 1991 (19). The procedure was performed after informed written consent was obtained from each patient. The study was approved by the medical ethics committee of the University of Leipzig Medical Center.

The pO_2 measurements in 17 premenopausal women with sporadic uterine leiomyomas were performed during surgery before any manipulation of the uterus (Table 1). Furthermore, pO_2 was also determined in the normal myometria of six premenopausal women who received surgery for gynecologic diseases other than leiomyoma and in one leiomyosarcoma. Patients underwent general anesthesia, whereby the oxygen content in the inspiratory air was reduced to 21% during pO_2 measurement procedures.

All pO_2 measurements were taken along at least two distinct electrode tracks within the macroscopically vital tumor or the normal uterine wall (myometrium). Per track, ≈36 readings were collected starting at a tissue depth of 5 mm, so that between 72 and 108 pO_2 readings were obtained per tumor. The median pO_2 and hypoxic fractions of all measured values were used to represent the oxygenation status of the respective tumor. Representative tissue samples, including the electrode tracks, were collected from all 17 measured leiomyomas during surgery.

Marker expression was also analyzed in nine leiomyosarcomas. Among these, eight cases were taken from archived paraffin material for which oxygenation data were not available. Both oxygenation status and marker expression were assessed in a single leiomyosarcoma (see above). All tissue samples were formalin-fixed and paraffin-embedded according to standard protocols before being evaluated by a gynecologic pathologist (L-C.H.).

Immunohistochemistry. Histologic slides were prepared from the paraffin blocks and dried overnight at 37°C. On the next day, specimens were dewaxed in two changes of fresh xylene and then rehydrated in a descending alcohol series. Retrieval of antigenic binding sites was performed by heating specimens in appropriate buffers (see Supplementary Table S1 for details) in a steamer (Braun FS 10, Braun) for 40 min. The primary antibodies and incubation conditions used are listed in Supplementary Table S1. Two different detection systems were applied: the standard streptavidin-biotin technique (DAKO Duet) was used for CA IX, Ki-67, GLUT-1, CD34, CD31, and HIF-2α. HIF-1α was detected with the catalyzed signal amplification system (DAKO CSA) to increase sensitivity. In the case of the streptavidin-biotin procedure (DAKO Duet), the biotinylated goat anti-mouse/anti-rabbit secondary antibody was applied for 30 min at 37°C followed by the streptavidin/biotin/horseradish peroxidase reagent in accordance with the manufacturer's instructions. Immunodetection with the DAKO CSA system (HIF-1α) was carried out following the manufacturer's instructions, except that all incubation steps were additionally temperature-controlled. Negative control specimens were incubated in PBS without the primary antibody under the same conditions. A tumor specimen with a known strong expression of each antigen was run as a positive control with every staining batch. Slides were counterstained with Mayer's hematoxylin, dehydrated in an ascending alcohol series, and covered with a coverslip using Eukitt mounting medium (Riedel-de Haen). Digital images of the specimens were acquired using a microscope-based image acquisition system consisting of a Zeiss Axiotron microscope (Zeiss) equipped with a PixeLINK PL-A686C (PixeLINK) camera connected to a standard Windows-based personal computer.

TUNEL assay. Apoptotic cells were detected by TUNEL. Slides were treated with the DeadEnd Colorimetric Apoptosis Detection System (Promega) according to the manufacturer's instructions. After deparaffinization (see above), sections were digested with proteinase K (20 mg/mL) for 5 min at 37°C and incubated with the reaction mixture (1:100) for 60 min at 37°C. This was followed by incubation with a streptavidin-peroxidase complex (1:500) for 30 min at room temperature and subsequent color development with 3,3′-diaminobenzidine (DAB). As positive controls, DNase-treated lymph node sections were used, and for negative controls, the TdT enzyme was omitted.

Table 1. Patient characteristics and tissue oxygenation status of uterine leiomyomas

Patient no.	Age (y)	Parity	Maximum leiomyoma diameter* (mm)	Median pO_2 (mm Hg)	HF 2.5 (%)	HF 5 (%)	HF 10 (%)
1	36	0	105	0.8	90	100	100
2	40	1	35	1.5	82	98	100
3	44	1	95	4.4	7	63	95
4	51	1	50	1.2	98	100	100
5	50	1	30	1.4	86	88	92
6	29	0	30	1.4	86	100	100
7	43	0	80	0.9	100	100	100
8	55	1	35	1.5	74	77	79
9	58	2	70	1.3	93	100	100
10	55	2	140	0.7	98	100	100
11	48	3	50	2.3	53	95	100
12	49	2	20	0.2	86	95	96
13	47	1	95	1.1	95	99	100
14	39	1	60	2.5	49	86	93
15	43	2	52	2.2	54	75	95
16	31	0	85	4.6	22	55	66
17	43	n.d.	n.d.	4.3	65	99	100

Abbreviations: HF 2.5, HF 5, and HF 10, hypoxic fraction or percentage of pO_2 readings below 2.5, 5, and 10 mm Hg, respectively; n.d., not determined.
*The maximum leiomyoma diameter was taken from the pathology report.

Evaluation of immunostaining. Although faint cytoplasmic or nuclear staining was also seen in some specimens, only distinct nuclear (HIF-1/HIF-2α, Ki-67, TUNEL) or membranous staining (GLUT-1, CA IX) was regarded as being evaluable as marker expression. Expression of hypoxia-associated markers was scored as being either absent or present. Ki-67 and TUNEL expression was scored using an image analysis–based system estimating the positive nuclear fraction, as described previously (20).

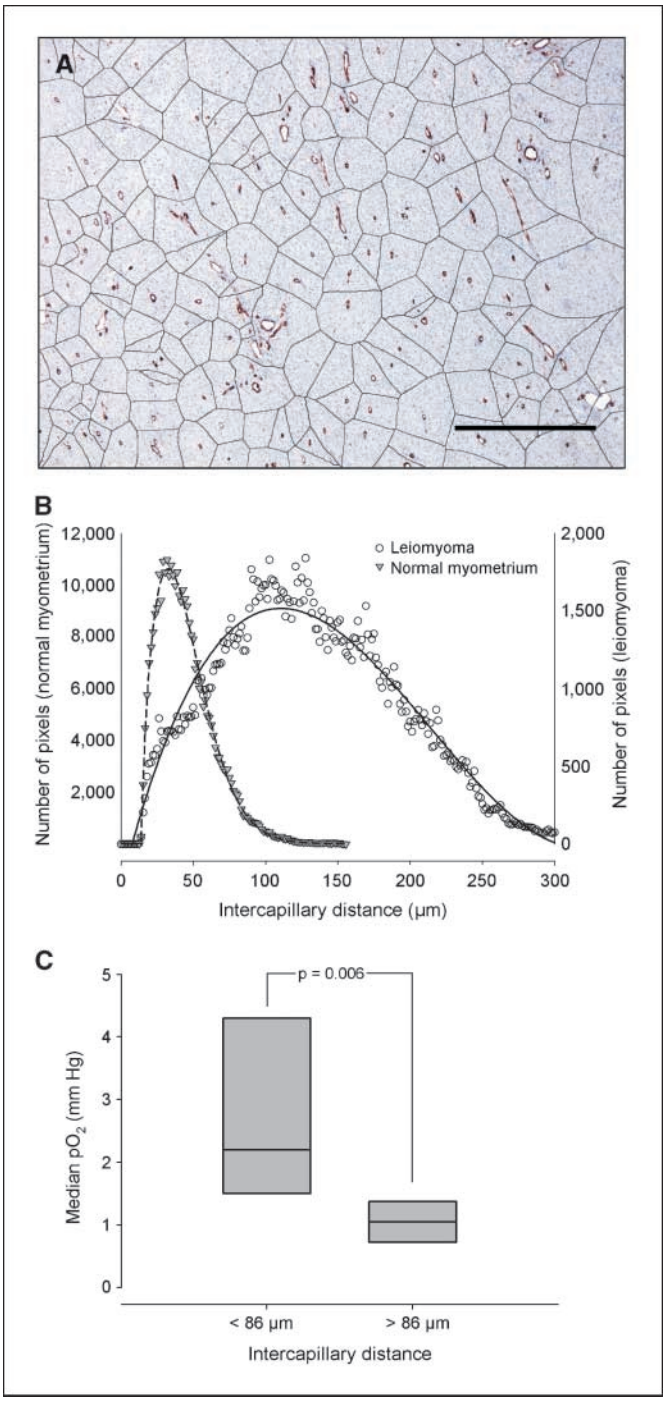

Figure 1. *A,* representative leiomyoma specimen stained with anti-CD34 antibody clone QBend 10 (DAB; *brown*). *Black,* vessel domain borders. *Scale bar,* 500 μm. *B,* ICD histogram from the image shown in *A* and of a specimen of normal myometrium. *C,* median pO_2 values in leiomyomas with small (*<86 μm*) and large (*≥86 μm*) ICDs. Significantly higher pO_2 values are found in the group with smaller ICD values. Note that no whiskers or symbols are shown because the number of cases was <10 in each group.

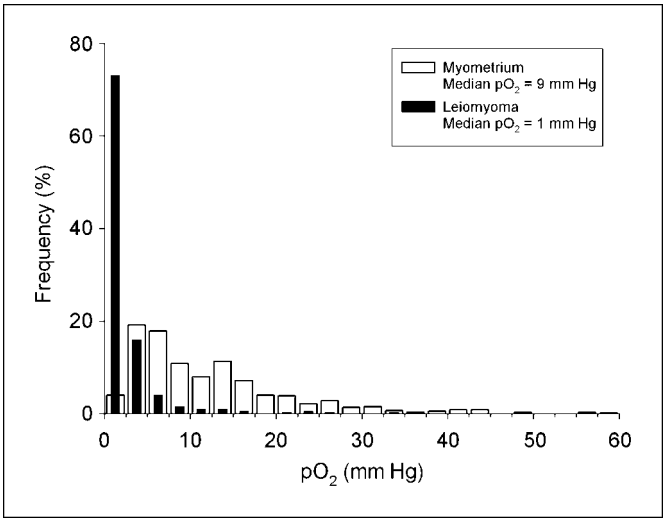

Figure 2. Distribution of oxygen partial pressures (pO_2) in normal myometrium (n = 6) and leiomyoma (n = 17).

Quantification of ICD. ICDs were measured in digital images of representative tumor areas (5× magnification; see Fig. 1*A*). Microvessels were identified by color thresholding of DAB-stained areas representing CD34/CD31 immunoreactivity using Optimas (Version 6.2; Media Cybernetics, Inc.). CD31 was substituted for CD34 in cases where CD34 staining was apparent in cell types other than endothelium. Thresholded pixels were converted to a binary image, in which pixels belonging to vessels were white (gray value, 255) and all other pixels were black (gray value, 0). The binary image was transferred to the freeware image processing tool ImageJ,[4] where it was converted to a Euclidean distance map, in which the gray value of each pixel is directly proportional to its distance from the nearest microvessel (i.e., to the white pixels in the transferred binary image) within an 8-bit dynamic range. This image was transferred back to Optimas and duplicated. A watershed transformation was applied to the duplicate image using a preflooding value of 10 pixels. This resulted in a second binary image showing only the borders (white, 255) between the microvessel domains; all other pixels were black (0). A third image was generated from the 8-bit distance map, and the binary microvessel domain border image by logically combining both images using the minimum operation. Accordingly, the white vessel domain borders were replaced by the gray values from the distance map. Modal ICDs were calculated from gray value histograms of these images (Fig. 1*B*). Figure 1*A* shows a composite image of a leiomyoma specimen stained with anti-CD34 (see Supplementary Table S1) and the microvessel domain borders (black lines). Due to the preflooding procedure of the watershed algorithm, only vessels of >10 pixels (≈14 μm) apart were considered to be separate. This step of the algorithm was implemented to minimize the erroneous separation of pixels belonging to identical vessel structures.

Statistical analysis. All statistical tests were performed using the SPSS software package (Version 14, SPSS, Inc.). The significance level was set at α = 5% for all comparisons. Linear correlations between two variables were described by Spearman's rank correlation coefficient (ρ). Two-sided Mann-Whitney U tests and Kruskal-Wallis tests were used for comparison of categorized variables. Survival estimates were calculated using the Kaplan-Meier method, and differences between groups were assessed with log-rank statistics.

Results

Oxygenation status. The oxygenation status was assessed by use of the Eppendorf pO_2 electrode in 17 leiomyomas, 6 cases of

[4] http://rsb.info.nih.gov/ij/

normal myometrium, and 1 leiomyosarcoma. The oxygenation data of the 17 uterine leiomyomas are presented in Table 1. A grand median pO_2 of 1 mm Hg (range, 0–5 mm Hg) was found, with individual oxygen partial pressures within each tumor varying between 1 and 50 mm Hg. Fifty percent of these benign tumors had a range of pO_2 values of <6 mm Hg. The median pO_2 of the leiomyosarcoma was 2 mm Hg. For normal myometria, the grand median pO_2 was 9 mm Hg (range, 5–20 mm Hg), which was significantly higher than that of the leiomyomas ($P < 0.0001$). A comparison of the distribution of the pO_2 values of normal myometrium ($n = 6$) and leiomyomas ($n = 17$; Fig. 2) showed that only 4% of the measurements were found in the lowest class (0–2.5 mm Hg) in the normal myometrium, whereas almost three quarters of the readings (≈73%) in leiomyomas were in this category indicating the most severe hypoxia.

Expression of HIF-1α/-2α, GLUT-1, and CA IX. Immunohistochemistry for HIF-1α/HIF-2α, CA IX, and GLUT-1 was performed in the leiomyomas, leiomyosarcomas, and normal myometria. All 17 leiomyomas and all normal myometria were negative for HIF-1α and HIF-2α, as well as for CA IX and GLUT-1. Figure 3*A* (*left*) shows an example of a leiomyoma found to be negative for GLUT-1; RBC served as endogenous positive controls. Figure 3*A* (*right*) shows perineural tissue found positive for GLUT-1 from a tissue area adjacent to leiomyoma cells. Validity of the immunodetection procedure of HIF-1/2α and CA IX was confirmed using exogenous controls (see Materials and Methods). HIF-1α expression was found in five of nine leiomyosarcomas (56%; Fig. 3*B, top left*). GLUT-1 (Fig. 3*B, top right*) and CA IX (Fig. 3*B, bottom left*) were expressed in the same seven of nine tumors (78%). With only one exception, each leiomyosarcoma overexpressed at least one hypoxia-associated marker protein. Expression of HIF-2α was found in all leiomyosarcomas, but was restricted to the tumor stroma, its expression being entirely absent from the tumor cells themselves (Fig. 3*B, bottom right*).

ICD. Modal ICD was assessed in 15 of 17 leiomyomas and ranged from 43 to 158 μm. Significantly higher median pO_2 values ($P = 0.006$) were found in tumors with a modal ICD below the median (86 μm; see Fig. 1*C*). Modal ICD values in the nine leiomyosarcomas ranged from 61 to 283 μm. The median of the modal ICD values was 68 μm. Both GLUT-1/CA IX–negative cases had a modal ICD of below 68 μm. The difference in ICD values between the leiomyomas and leiomyosarcomas was not statistically significant. The median value of the modal ICD in

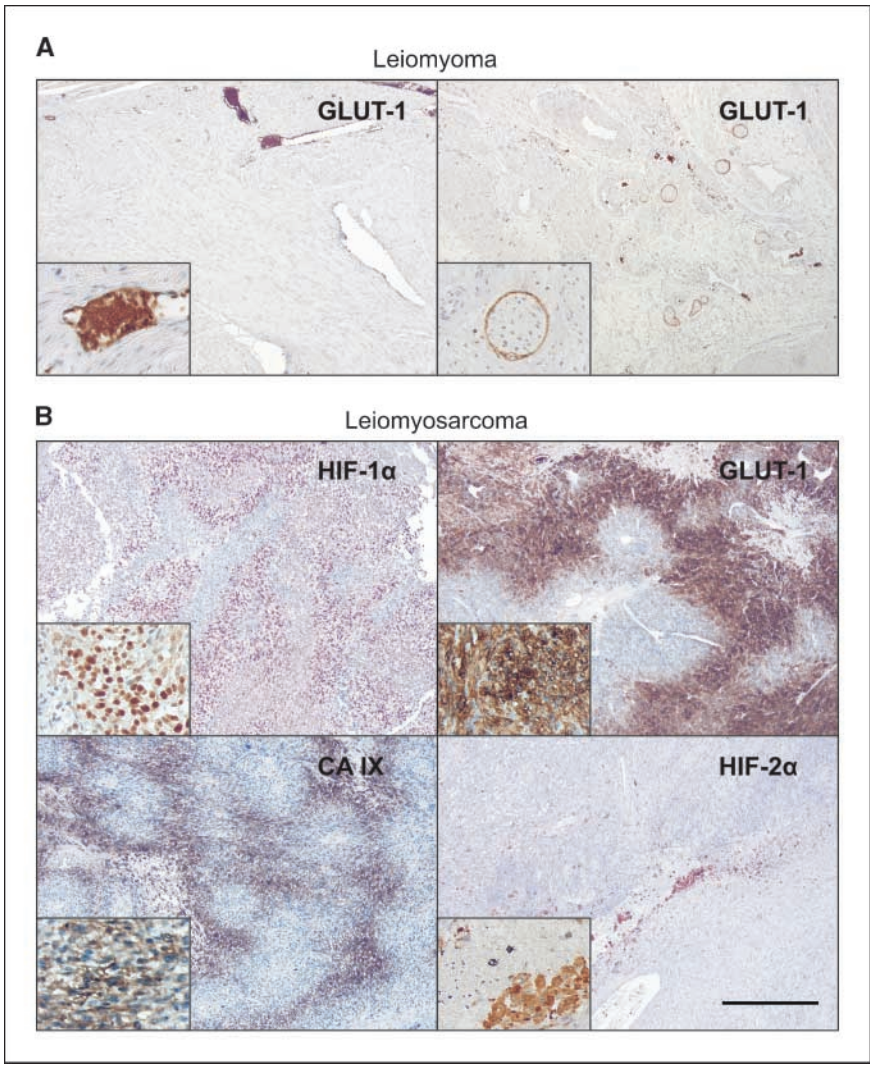

Figure 3. *A,* hypoxia-related markers in leiomyoma. *Left,* leiomyoma cells negative for GLUT-1. RBCs within vessel lumina serve as endogenous positive controls. *Right,* perineural sheath tissue staining positive for GLUT-1. *B,* various leiomyosarcomas positive for HIF-1α (*top left*), GLUT-1 (*top right*), CA IX (*bottom left*); cellular elements in the stroma of a leiomyosarcoma specimen positive for HIF-2α (*bottom right*). The scale bar in the lower right corner corresponds to a length of 500 μm and applies to all panels (magnification, 5×). The insets show details of the staining patterns at higher (40×) magnification.

normal myometrium was 42 μm (range, 29–62 μm), i.e., significantly smaller than in the leiomyomas (P = 0.0001) and leiomyosarcomas (P = 0.0001).

Proliferation and apoptosis. Ki-67 labeling (Fig. 4*A*) and apoptosis detection using the TUNEL assay (AI; Fig. 4*B*) were carried out in 16 of the 17 leiomyomas and in nine leiomyosarcomas. The Ki-67 labeling index was significantly lower in the leiomyomas (median, 3.85%; range, 1.0–15.9%) when compared with the leiomyosarcomas (median, 21.4%; range, 0.4–55.8%; P = 0.004). The apoptotic indices for the leiomyomas (median, 0.1%; range, 0–0.3%) were also significantly lower than those of the leiomyosarcomas (median, 1.8%; range, 0–29%; P = 0.004). Figure 4*C* illustrates these differences. No correlations were found between proliferation or apoptosis and the oxygenation status or modal ICD.

Discussion

Proliferating uterine leiomyomas in premenopausal women exhibit extremely low pO_2 values. Although such oxygenation profiles would be classified as "severely hypoxic" when compared with pO_2 distributions in normal tissues and in solid malignant tumors, markers of the hypoxic response (HIF-1α/HIF-2α, GLUT-1, and CA IX) were not detected. In contrast, hypoxia-associated markers were found to be abundantly expressed in leiomyosarcomas. Oxygenation data were only available for one leiomyosarcoma, which was hypoxic. These findings were unexpected because the induction of HIF-1α and its target genes is generally perceived as being a physiologic reaction to hypoxia, occurring independently of malignant transformation. Because cycles of hypoxia and reoxygenation have been shown to be of importance, e.g., in metastasis (21, 22), it is worth noting that leiomyomas additionally exhibited an exceedingly low intratumoral variation in tissue oxygenation, which could be indicative of only flat spatio-temporal oxygen gradients. Indeed, we need to consider the possibility that a pronounced variability in oxygenation—as evident in many solid malignancies—may in fact be an even more prominent factor in terms of tumor progression than a severe but stable hypoxic microenvironment.

It is unlikely that these results are the consequence of methodological problems associated with our immunohistochemical techniques. The detection of HIF-1α using the antibody clone H1α67 in conjunction with a biotinyl-tyramide–based signal amplification system as first described by Zhong and colleagues (23) is well-established. This technique has been used by ourselves and others and has been shown to consistently yield plausible staining patterns (20, 24). Positive control specimens show clear nuclear staining that is found to be more intense with increased distance from microvessels. The validity of the GLUT-1 staining can be seen from the constitutively positive RBC and perineural tissue, which served as endogenous controls (ref. 25; see Fig. 3*A*). As pointed out in Materials and Methods, positive control specimens were carried out for all antigens with every staining batch.

Expression of HIF-1α has been shown in leiomyomas from patients with the rare syndrome of hereditary leiomyoma and renal cell cancer (HLRCC; ref. 26). Compared with the normal myometrium, tumors arising in this condition have been shown to be hypervascular (27) and exhibit a substantially increased risk for the development of leiomyosarcoma (71-fold; see ref. 28). The pathogenetic basis of this disease is an inactivating mutation of the tricarbonic acid cycle enzyme fumarate hydratase, which leads to accumulation of fumarate. This metabolite inhibits prolyl hydroxylases and consequently leads to HIF-1α stabilization secondary to decreased proteasomal degradation (29). Unfortunately, no material from HLRCC patients could be included in the present study. The assessment of the oxygenation status in HLRCC

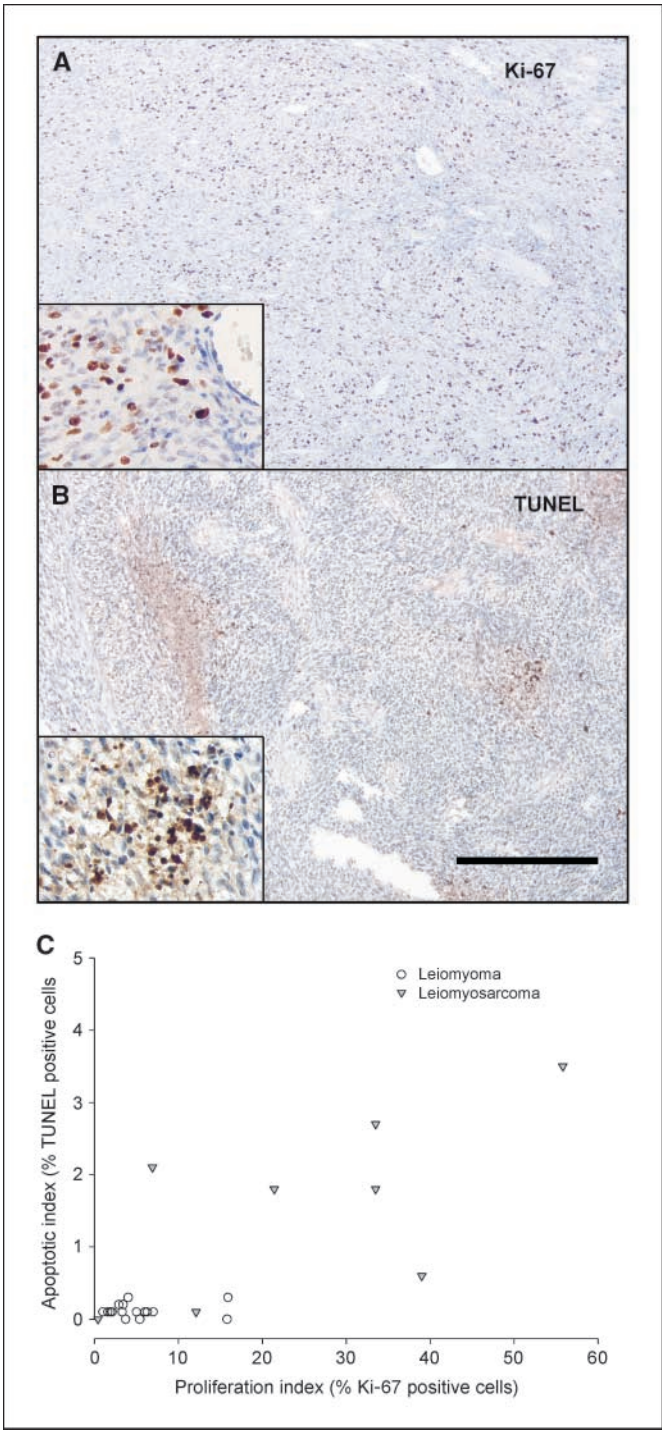

Figure 4. Examples of Ki-67 (*A*) and TUNEL (*B*) immunohistochemistry. *Scale bar,* 500 μm (magnification, 5×). *Insets,* 40× magnification. *C,* leiomyosarcomas (*triangles*) show significantly higher proliferation and apoptosis values than the leiomyomas (*circles*). One leiomyosarcoma with an exceptionally high apoptotic index of ~29% is located outside the scaling of this diagram.

tumors would, however, certainly be an interesting subject for further studies.

The findings presented here in sporadic leiomyoma are in agreement with those of an earlier study by Zhong and colleagues (23), who showed the absence of HIF-1α expression in 12 benign tumor specimens (10 fibroadenomas of the breast and 2 leiomyomas of the uterus). Likewise, Younes and colleagues (30) assessed the expression of GLUT-1 in a wide array of normal (and cancerous) tissues and found leiomyomas, as well as several other benign tumor entities (among them adenomas of the colon and liver and prostatic hyperplasia), to all be negative. To our knowledge, the expression of CA IX or HIF-2α has not been previously investigated in these benign tumor entities. Indeed, immunohistochemical studies examining the expression of hypoxia-related markers in leiomyoma (and other benign human tumors) are rare.

Compared with normal myometrium, the oxygenation of leiomyomas was significantly poorer and they were also less vascularized (i.e., they exhibited a larger ICD). Although the oxygenation status of leiomyomas showed only minimal intertumoral variation, significantly lower median pO_2 values in tumors with ICD values above the median were found. Proliferation and apoptosis were very low, consistent with a chronically hypoxic, diffusion-limited system. These data may indicate that leiomyoma growth—although partially autonomous—is still restricted by oxygen availability. Whereas in terms of absolute pO_2 values they are classified as being hypoxic, leiomyoma cells may however not experience hypoxic stress. In fact, mechanisms matching the oxygen demand for anabolic processes to highly restrained oxygen availability may be active in leiomyoma, resulting in a balanced, low-level bioenergetic state. Such mechanisms may be fundamental for benign tumor growth in general, explaining the lack of hypoxia-related marker expression found in this and other studies.

A central regulator of anabolic processes and cell growth in eukaryotic cells is the serine/threonine kinase mammalian target of rapamycin (mTOR; for a review, see ref. 31). Activation of mTOR is the final common pathway for growth factor signaling through receptor tyrosine kinases and downstream phosphatidylinositol-3-kinase (PI3K) and rat sarcoma (RAS) pathways. mTOR matches these stimulatory signals to nutrient availability in the microenvironment (32), and it is becoming increasingly evident that oxygen availability plays a central role in this regulation. Repression of mTOR signaling under hypoxia could thus be a key element in a feedback mechanism that results in an adapted bioenergetic status in the hypoxic microenvironment of leiomyomas. Hypoxia activates the TSC-1/2 (hamartin/tuberin) complex via sensing proteins,

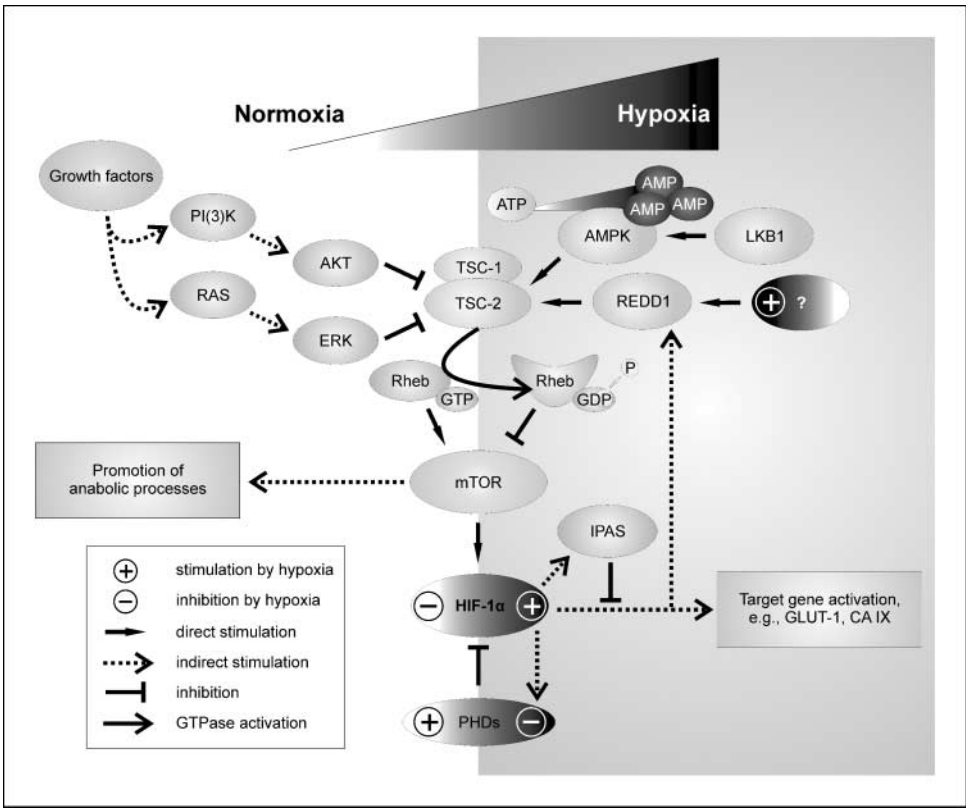

Figure 5. Negative feedback mechanisms on HIF-1α signaling under chronic hypoxia with special emphasis on mTOR. In normoxia (*left, white background*), HIF-1α protein synthesis is up-regulated by growth factor signaling via PI3K/AKT and RAS/extracellular signal-regulated kinase (*ERK*) pathways through inhibition of the TSC-1/TSC-2 complex and consecutive activation of mTOR by GTP-bound Rheb. mTOR also stimulates anabolic processes at multiple levels. Hypoxia (*right, light gray background*) activates the TSC-1/TSC-2 complex by activating AMPK and REDD1. Both proteins increase the GTPase activity of Rheb, leading to its conversion to the GDP-bound state, a change in protein conformation and suppression of mTOR signaling. Activation of TSC-1/TSC-2 by hypoxia may be partially HIF-1α dependent (via transactivation of REDD1) and partially HIF-1α independent. The latter pathway involves the phosphorylation of AMPK by LKB1 in the presence of AMP and possibly a direct effect of hypoxia on REDD1 activity via undefined upstream signaling processes. HIF-1α also promotes its own degradation by induction of prolyl hydroxylases, which—despite being most effective when O_2 levels are high—remain partially active under hypoxia. Gray level gradients correspond to oxygen gradients, with the darkest areas representing the most severely hypoxic status. See text for additional details, and abbreviations, respectively. The diagram is an extended and modified version of a diagram presented earlier by Pouysségur and colleagues (37).

which may include AMP-activated protein kinase (AMPK; ref. 33) or regulated in development and DNA damage responses 1 (REDD1; ref. 34). The TSC-1/TSC-2 complex is a GTPase activator for the small GTPase RAS homologue enriched in brain (Rheb), promoting Rheb inactivation (a common principle in the regulation of G protein–coupled signaling). Because mTOR is dependent on stimulation by Rheb, hypoxia may down-regulate its activity via this pathway. In addition to being a crucial event leading to reduced cell growth, inhibition of mTOR has also been shown to lead to the direct down-regulation of HIF-1α at the level of mRNA translation (35) or protein stability (36), in line with our findings in leiomyomas. Diagrams illustrating these mechanisms have been presented recently (32, 37), and elements relevant to this discussion have been compiled within Fig. 5. Further feedback mechanisms of hypoxia on HIF-1α expression have also been identified. Prolonged hypoxia leads to the up-regulation of prolyl hydroxylase isoenzymes 2 and 3 (38), whereby the former is a direct target of HIF-1α (39). Moreover, transactivational activity of HIF-1α was shown to be inhibited by the dominant-negative regulator inhibitory Per/Arnt/Sim domain protein (40), which is also a direct HIF-1α target, thus again constituting a negative feedback loop.

The paradigm that hypoxia must invariably lead to HIF-1α induction is challenged by our findings. It may at least partially stem from the fact that many studies assessed the behavior of transformed cells under *in vitro* conditions (e.g., refs. 41, 42). Bearing in mind the complete absence of hypoxia-related markers found in leiomyomas, the negative feedback effect of mTOR and similar mechanisms on the activation of the hypoxic response in benign tissues may currently be underestimated.

Dysregulation of mTOR signaling is a common finding in malignant cells, e.g., as a consequence of activating mutations in the PI3K and RAS signaling pathways. mTOR activation may indeed be of particular importance for smooth muscle cell transformation, because mice carrying deletions of the tumor suppressor PTEN (an endogenous antagonist of PI3K signaling) develop widespread smooth muscle cell hyperplasia and abdominal leiomyosarcomas (43). In our study, proliferation and apoptosis were significantly higher in leiomyosarcoma compared with leiomyoma, regardless of a similar modal ICD. This high-turnover phenotype under microenvironmental conditions, which are comparable with those found in leiomyoma, would be compatible with a situation in which hypoxia is unable to suppress mTOR-mediated stimulation of cell growth. Additionally, almost all leiomyosarcomas expressed one or more hypoxia-related markers. Because the expression of such markers is also under the control of mTOR (see above), the same molecular network that allows cells to proliferate under low oxygen microenvironmental conditions may enable the activation of the hypoxic response. The negative feedback of hypoxia on the HIF system (which is likely to include elements other than mTOR) seems to be organized in a dichotomous rather than a gradual fashion. Therefore, we postulate that a hypoxic switch, which allows cells to proliferate independently of the restraints of available oxygen resources, is a key element of malignancy. This capability—hazardous in its own right—will eventually lead to a detrimental reduction in the bioenergetic status and to a consecutive strong activation of the hypoxic response program with serious consequences for the host in terms of aggressive tumor cell behavior.

In conclusion, evidence has been presented that, despite the presence of extreme hypoxia, the HIF system is not active in benign uterine leiomyomas. Their malignant counterparts, leiomyosarcomas, are characterized by a strong induction of hypoxia-related markers. These findings are compatible with a pathophysiologic model in which hypoxic stress, arising from proliferation that is not restricted by the availability of resources, seems to be a main driving force behind the malignant phenotype.

Disclosure of Potential Conflicts of Interest

No potential conflicts of interest were disclosed.

Acknowledgments

Received 11/27/2007; revised 3/10/2008; accepted 3/17/2008.

Grant support: Deutsche Krebshilfe grant 106758.

The costs of publication of this article were defrayed in part by the payment of page charges. This article must therefore be hereby marked *advertisement* in accordance with 18 U.S.C. Section 1734 solely to indicate this fact.

We thank Dr. Debra Kelleher for her excellent editorial assistance.

References

1. Höckel M, Knoop C, Schlenger K, et al. Intratumoral pO_2 predicts survival in advanced cancer of the uterine cervix. Radiother Oncol 1993;26:45–50.
2. Höckel M, Schlenger K, Aral B, Mitze M, Schäffer U, Vaupel P. Association between tumor hypoxia and malignant progression in advanced cancer of the uterine cervix. Cancer Res 1996;56:4509–15.
3. Nordsmark M, Overgaard M, Overgaard J. Pretreatment oxygenation predicts radiation response in advanced squamous cell carcinoma of the head and neck. Radiother Oncol 1996;41:31–9.
4. Brizel DM, Scully SP, Harrelson JM, et al. Tumor oxygenation predicts for the likelihood of distant metastases in human soft tissue sarcoma. Cancer Res 1996;56:941–3.
5. Plate KH, Breier G, Millauer B, Ullrich A, Risau W. Up-regulation of vascular endothelial growth factor and its cognate receptors in a rat glioma model of tumor angiogenesis. Cancer Res 1993;53:5822–7.
6. Graeber TG, Osmanian C, Jacks T, et al. Hypoxia-mediated selection of cells with diminished apoptotic potential in solid tumours. Nature 1996;379:88–91.
7. Pennacchietti S, Michieli P, Galluzzo M, Mazzone M, Giordano S, Comoglio PM. Hypoxia promotes invasive growth by transcriptional activation of the met protooncogene. Cancer Cell 2003;3:347–61.
8. Bedogni B, Welford SM, Cassarino DS, Nickoloff BJ, Giaccia AJ, Powell MB. The hypoxic microenvironment of the skin contributes to Akt-mediated melanocyte transformation. Cancer Cell 2005;8:443–54.
9. Erler JT, Bennewith KL, Nicolau M, et al. Lysyl oxidase is essential for hypoxia-induced metastasis. Nature 2006;440:1222–6.
10. Höckel M, Vaupel P. Tumor hypoxia: definitions and current clinical, biologic, and molecular aspects. J Natl Cancer Inst 2001;93:266–76.
11. Harris AL. Hypoxia-a key regulatory factor in tumour growth. Nat Rev Cancer 2002;2:38–47.
12. Gatenby RA, Gillies RJ. Why do cancers have high aerobic glycolysis? Nat Rev Cancer 2004;4:891–9.
13. Semenza GL. Targeting HIF-1 for cancer therapy. Nat Rev Cancer 2003;3:721–32.
14. Denko NC, Fontana LA, Hudson KM, et al. Investigating hypoxic tumor physiology through gene expression patterns. Oncogene 2003;22:5907–14.
15. Potter CP, Harris AL. Diagnostic, prognostic and therapeutic implications of carbonic anhydrases in cancer. Br J Cancer 2003;89:2–7.
16. Wallach EE, Vlahos NF. Uterine myomas: an overview of development, clinical features, and management. Obstet Gynecol 2004;104:393–406.
17. Stewart EA, Morton CC. The genetics of uterine leiomyomata: what clinicians need to know. Obstet Gynecol 2006;107:917–21.
18. Sandberg AA. Updates on the cytogenetics and molecular genetics of bone and soft tissue tumors: leiomyosarcoma. Cancer Genet Cytogenet 2005;161:1–19.
19. Höckel M, Schlenger K, Knoop C, Vaupel P. Oxygenation of carcinomas of the uterine cervix: evaluation by computerized O_2 tension measurements. Cancer Res 1991;51:6098–102.
20. Mayer A, Wree A, Höckel M, Leo C, Pilch H, Vaupel P. Lack of correlation between expression of HIF-1a protein and oxygenation status in identical tissue areas of squamous cell carcinomas of the uterine cervix. Cancer Res 2004;64:5876–81.
21. Cairns RA, Kalliomaki T, Hill RP. Acute (cyclic) hypoxia enhances spontaneous metastasis of KHT murine tumors. Cancer Res 2001;61:8903–8.
22. Rofstad EK, Galappathi K, Mathiesen B, Ruud EB. Fluctuating and diffusion-limited hypoxia in hypoxia-induced metastasis. Clin Cancer Res 2007;13:1971–8.
23. Zhong H, De Marzo AM, Laughner E, et al.

Overexpression of hypoxia-inducible factor 1a in common human cancers and their metastases. Cancer Res 1999;59:5830–5.
24. Aebersold DM, Burri P, Beer KT, et al. Expression of hypoxia-inducible factor-1a: a novel predictive and prognostic parameter in the radiotherapy of oropharyngeal cancer. Cancer Res 2001;61:2911–6.
25. Mayer A, Höckel M, Wree A, Vaupel P. Microregional expression of glucose transporter-1 and oxygenation status: lack of correlation in locally advanced cervical cancers. Clin Cancer Res 2005;11:2768–73.
26. Pollard PJ, Briere JJ, Alam NA, et al. Accumulation of Krebs cycle intermediates and over-expression of HIF1a in tumours which result from germline FH and SDH mutations. Hum Mol Genet 2005;14:2231–9.
27. Pollard P, Wortham N, Barclay E, et al. Evidence of increased microvessel density and activation of the hypoxia pathway in tumours from the hereditary leiomyomatosis and renal cell cancer syndrome. J Pathol 2005;205:41–9.
28. Lehtonen HJ, Kiuru M, Ylisaukko-oja SK, et al. Increased risk of cancer in patients with fumarate hydratase germline mutation. J Med Genet 2006;43:523–6.
29. Isaacs JS, Jung YJ, Mole DR, et al. HIF overexpression correlates with biallelic loss of fumarate hydratase in renal cancer: novel role of fumarate in regulation of HIF stability. Cancer Cell 2005;8:143–53.
30. Younes M, Lechago LV, Somoano JR, Mosharaf M, Lechago J. Wide expression of the human erythrocyte glucose transporter Glut1 in human cancers. Cancer Res 1996;56:1164–7.
31. Wullschleger S, Loewith R, Hall MN. TOR signaling in growth and metabolism. Cell 2006;124:471–84.
32. Shaw RJ, Cantley LC. Ras, PI3K and mTOR signalling controls tumour cell growth. Nature 2006; 441:424–30.
33. Liu L, Cash TP, Jones RG, Keith B, Thompson CB, Simon MC. Hypoxia-induced energy stress regulates mRNA translation and cell growth. Mol Cell 2006;21: 521–31.
34. Brugarolas J, Lei K, Hurley RL, et al. Regulation of mTOR function in response to hypoxia by REDD1 and the TSC1/TSC2 tumor suppressor complex. Genes Dev 2004;18:2893–904.
35. Laughner E, Taghavi P, Chiles K, Mahon PC, Semenza GL. HER2 (neu) signaling increases the rate of hypoxia-inducible factor 1a (HIF-1a) synthesis: novel mechanism for HIF-1-mediated vascular endothelial growth factor expression. Mol Cell Biol 2001;21:3995–4004.
36. Hudson CC, Liu M, Chiang GG, et al. Regulation of hypoxia-inducible factor 1a expression and function by the mammalian target of rapamycin. Mol Cell Biol 2002; 22:7004–14.
37. Pouysségur J, Dayan F, Mazure NM. Hypoxia signalling in cancer and approaches to enforce tumour regression. Nature 2006;441:437–43.
38. Marxsen JH, Stengel P, Doege K, et al. Hypoxia-inducible factor-1 (HIF-1) promotes its degradation by induction of HIF-a-prolyl-4-hydroxylases. Biochem J 2004;381:761–7.
39. Metzen E, Stiehl DP, Doege K, Marxsen JH, Hellwig-Burgel T, Jelkmann W. Regulation of the prolyl hydroxylase domain protein 2 (phd2/egln-1) gene: identification of a functional hypoxia-responsive element. Biochem J 2005;387:711–7.
40. Makino Y, Uenishi R, Okamoto K, et al. Transcriptional up-regulation of inhibitory PAS domain protein gene expression by hypoxia-inducible factor 1 (HIF-1): a negative feedback regulatory circuit in HIF-1-mediated signaling in hypoxic cells. J Biol Chem 2007;282:14073–82.
41. Jiang BH, Semenza GL, Bauer C, Marti HH. Hypoxia-inducible factor 1 levels vary exponentially over a physiologically relevant range of O_2 tension. Am J Physiol 1996;271:C1172–80.
42. Jewell UR, Kvietikova I, Scheid A, Bauer C, Wenger RH, Gassmann M. Induction of HIF-1a in response to hypoxia is instantaneous. FASEB J 2001;15:1312–4.
43. Hernando E, Charytonowicz E, Dudas ME, et al. The AKT-mTOR pathway plays a critical role in the development of leiomyosarcomas. Nat Med 2007;13: 748–53.

Lack of Hypoxic Response in Uterine Leiomyomas despite Severe Tissue Hypoxia

Arnulf Mayer, Michael Höckel, Alexander Wree, et al.

Cancer Res 2008;68:4719-4726.